Meteorological and soil surface effects in gamma radiation time series - implications for assessment of earthquake precursors

Susana Barbosa[a], Johan Alexander Huisman[b], Eduardo Brito Azevedo[c]

[a] *INESC TEC, CSIG - Centre of Information Systems and Computer Graphics, Portugal*
[b] *Agrosphere Institute (IBG-3), Forschungszentrum Jlich GmbH, Juelich, Germany*
[c] *Center of Climate Meteorology and Global Change, University of the Azores*

Abstract

Monitoring of environmental radioactivity for the purpose of earthquake prediction requires the discrimination of anomalies of non-tectonic origin from seismically-induced anomalies. This is a challenging task as time series of environmental radioactivity display a complex temporal pattern reflecting a wide range of different physical processes, including meteorological and surface effects. The present study is based on the detailed time series of gamma radiation from the Eastern North Atlantic (ENA) site in the Azores, and on very high resolution precipitation intensity and soil moisture time series. The results show that an abrupt shift in the average level of the gamma radiation time series previously reported as a potential earthquake precursor can also be explained by a corresponding abrupt change in soil moisture. It was concluded that the reduction of false positive earthquake precursors requires the detailed assessment of both precipitation and soil moisture conditions at high temporal resolution.

Keywords: gamma radiation, earthquakes, precipitation, soil moisture

---

Postprint of paper published in Journal of Environmental Radioactivity.

DOI:https://doi.org/10.1016/j.jenvrad.2018.09.022

1. Introduction

Radon (Rn-222) is considered a potential earthquake precursor based on diverse laboratory experiments showing that radon is released during rock fracturing (Holub & Brady, 1981; Mollo et al., 2011; Nicolas et al., 2014). It has also been shown that the connection of initially isolated cracks in crustal rocks before rupture can cause a release of radon transients measurable at the surface (Girault et al., 2017). However, the majority ($\sim$90%) of preseismic anomalies in radon concentration are not associated with seismic activity but rather with meteorological, hydrological, and environmental conditions (Jordan et al., 2011). Therefore, it is crucial for the application of radon as a geodynamic proxy to identify the origin of radon anomalies, which is a challenging task as anomalies of non-tectonic origin can be strikingly similar to seismo-tectonically induced radon anomalies(Woith, 2015; Arora et al., 2017)).

The investigation of radon as a potential earthquake precursor requires long and continuous time series of field measurements. The long-term monitoring of Rn-222 at high temporal resolution can be performed using solid detectors or ionization chambers counting the alpha particles from radon decay, or alternatively by counting the gamma rays emitted by radon progeny. Crystal scintillators for gamma ray detection are advantageous for long-term monitoring in stable subsurface conditions due to their significantly higher capability to resolve temporal variations and ability to monitor directly short-term radon variations within the geological media, without the time delay required for the radon to move and reach equilibrium within the air volume sensed by the alpha detector (Zafrir et al., 2011). Thus, gamma-ray detection systems can be useful for long-term monitoring for earthquake prediction purposes.

Anomalous variations in the temporal variability of gamma-ray counting rates have been reported preceding earthquake events (e.g. Tsvetkova et al. (2001, 2014); Fu et al. (2015); Novikov et al. (2016)). However, gamma radiation typically displays a complex temporal pattern, and equally strong variations can be also found in the absence of earthquakes. Thus, it is fundamental to examine not only the association between anomalies in gamma radiation and earthquake events, but to also consider the whole temporal variability of gamma radiation and its relation to meteorological factors, including both atmospheric and surface effects. The temporal variability of gamma radiation is well known to be strongly influenced by precipitation (e.g Inomata et al. (2007); Mercier et al. (2009); Bossew et al. (2017); Melintescu et al. (2018)) and by the soil water content (Carroll, 1981). A further influence is radon build-up within the stable boundary layer (e.g. Chambers et al. (2011)).

The present study illustrates the relevance of considering simultaneously meteorological and soil surface conditions when assessing potential earthquake precursory signs in gamma radiation time series. Based on a detailed record from the gamma radiation monitoring campaign at the Eastern North Atlantic (ENA) site in the Azores (Barbosa et al., 2017), this work focuses on a previously reported potential earthquake precursor (Barbosa et al., 2016), and how it can actually be explained by a combination of very specific meteorological and surface conditions at the monitoring site.

2. Material and methods

2.1. Geographic setting

The Eastern North Atlantic (ENA) facility is a permanent ARM (Atmospheric Radiation Measurement) site installed at the Graciosa Island (39°N, 28° W) of the Azores archipelago in the middle of the North Atlantic Ocean (Fig. 1). The location is unique from a geophysical point of view because it is located at the Azores triple junction of the Eurasian, North American, and African plates in a seismically and volcanically active area (Hildenbrand et al., 2014; Hipólito et al., 2014). The ENA station is located in the northern part of the Graciosa Island, situated in the northwestern tip of the slow-spreading Terceira rift separating the Eurasian plate to the North from the Nubian plate to the south (Vogt & Jung, 2004).

The climate of Graciosa is dictated by its geographical setting and its interaction with the surrounding sea, as well as by its size and altitude. From its position north of the central group of islands of the Azores, the island is very well exposed to the path of the intense meteorological activity that occurs along the Polar Front, crossing the archipelago by north from west to the east. The prevailing winds at the ENA site are also West-East. Due to its small dimension (only 61 square kilometers) and low altitude (only 402 meters high), the island does not interfere much with the marine boundary layer above, which led to the choice of Graciosa for the installation of the ENA facility (Nitschke & de Azevedo, 2015). According to the Köppen climate classification, the littoral climate of Graciosa is included in the temperate climates category with oceanic features (group Csb). It is characterized by having a summer and a winter, average annual temperature above 17°C, and annual average precipitation of 845 mm at sea level. Due to its lower altitude, Graciosa Island is one of the more sunny islands of the archipelago and also the one with less ability to produce orographic rain, making it one of the most driest islands of the Azores (Azevedo, 2015).

The soil of Graciosa reflects the volcanic origin of the island, being mainly derived from the evolution of tephra and basaltic rock in the mild and humid climate of the Atlantic (Madruga et al., 2015).

2.2. Monitoring set-up

Gamma radiation is continuously monitored at the ENA station since May 2015 in the framework of the Gamma Radiation Monitoring campaign. The gamma detector is a NaI(Tl) scintillator (Scionix, the Netherlands) equipped with an electronic total count Single Channel Analyzer (SCA) that detects gamma radiation in the energy range from 475 keV to 3 MeV in order to reduce the Compton background in the 50-475 keV low-energy range (Zafrir et al., 2011). The sensor is installed inside a metal container at 1 m above ground with the scintillation head facing upwards.

2.3. Data

The gamma radiation data consist of a time series of total gamma-ray counts with a 15-minute temporal resolution that has been collected since 2015/05/08 in counts per minute (cpm). The measurements were performed every 15-minutes from May 2015 to April 2016, and then every 1-minute since May 2016. For consistency between the two measurement periods, the time series considered hereafter consists of 15-min counts from the 1st period and the counts resulting from the temporal aggregation (sum) of the 1-min counts from the 2nd period. The data is publicly available at the ARM archive (https://doi.org/10.5439/1441191) and can be also freely obtained from a CKAN repository (https://rdm.inesctec.pt).

Precipitation and soil moisture data are routinely measured at the ARM-ENA facility, and they are freely available from the ARM data archive. Precipitation data are obtained from laser disdrometer measurements (Parsivel2, Germany) every 1-minute. Soil moisture data is obtained from SEBS (Surface Energy Balance System) measurements using a capacitive sensor (SMP1, Radiation and Energy Balance Systems, Inc.) yielding soil water potential from temperature-corrected resistance measurements. The soil water potential is further converted to gravimetric soil moisture using a generic soil water characteristic equation and assuming a very fine sandy loam as the soil type (Cook, 2016). The resulting values of soil moisture are available at 5 cm, 10 cm and 15 cm depths with a temporal resolution of 30 minutes. In this study, the soil moisture time series are further re-scaled to an arbitrary range between 0 (dry) and 1 (wet) corresponding to the daily minimum and maximum values of the time series.

3. Results

3.1. Gamma radiation

The time series of gamma counts from the gamma monitoring campaign at ENA is shown in Fig. 2 for the year 2015. The time series displays very sharp peaks, typically lasting < 6 hours, which are more frequent and of higher magnitude from mid-September to December. These sharp peaks are associated with concurrent precipitation events (Barbosa et al., 2017) and result mainly from the deposition of radon progeny, Pb-214 and Bi-214 (Livesay et al., 2014).

The time series of gamma counts shows an apparent break in the mean level in mid-August 2015. The break is confirmed by the Mann-Whitney non-parametric test for detecting shifts in the mean (Ross, 2015), which identifies a small ($< 2\%$) but statistically significant change in the mean level of counts from 7564 cpm to 7440 cpm on 26th August 2015 at 02h45 (vertical dashed line in Fig. 2). Figure 3 shows a zoom of the time series of gamma counts and precipitation rate around the identified breakpoint on 26th August. The meteorological conditions are dominated by the passage of a frontal system with strong precipitation occurring on August 26th from 00h00 to about 04h00. The decrease in gamma radiation starts before the occurrence of the most intense precipitation at 03h15, which seems to reduce the rate of decrease of gamma counts. Strong precipitation is associated with enhanced radiation at ground level as a result of precipitation scavenging of radon progeny (e.g. Paatero & Hatakka (1999); Livesay et al. (2014); Yakovleva et al. (2016)), but in this case the rain at 03:15 rather than enhancing seems to slow down the decrease in gamma counts. While typically at the ENA site the enhancement in gamma radiation resulting from strong precipitation is followed by lower counts due to increased soil saturation (Barbosa et al., 2017), the effect typically lasts for some hours after the rain event. In this case however the level of gamma radiation remained lower than before the shift for several months, and relatively stable until the end of the year, suggesting an alternative origin. The fact that an earthquake occurred in the area at approximately the same time as the identified shift in gamma radiation led to the suggestion that the shift in gamma radiation could be associated with that seismic event (Barbosa et al., 2016).

3.2. Seismicity

Seismic information for the study area (31.5°W to 24.5°W, 36.5°N to 40.5°N) is obtained from the EMSC (European-Mediterranean Seismological Centre) catalog and from IPMA (Instituto Português do Mar e da Atmosfera) seismic bulletins. All the earthquakes occurring in the region from the 8th of May to December 31st, the period coincident with the gamma radiation monitoring in 2015, are selected from the catalogs and displayed in Figure 4. An earthquake of magnitude ML3.3 (marked by an X in Fig. 4) occurred on 2015/08/26, the same day as the level shift in gamma radiation. The earthquake happened at 02h16, about 30 minutes before the identified shift in the gamma radiation. However, it is not the strongest event or the closest to the monitoring site. A shallow event of the same magnitude (ML 3.3) and very near the location of the earthquake of 26th of August occurred later (October 23th) with no apparent change in the gamma radiation level.

Figure 5 shows the time series of gamma radiation (every 15-minutes) along with precipitation intensity (every 1-minute) and wind information (wind direction and average wind speed) for the day of occurrence of the largest earthquake events (ML $\geq$ 3.5). The availability of very high temporal resolution precipitation data allows to see clearly that the anomalies in gamma radiation before the ML3.9 earthquake on May 8th 2015 and the ML3.6 earthquake on December 24th are related to intense precipitation and corresponding scavenging of radon progeny. The strong precipitation in the evening of June 29th is of thermal convection origin and thus not affects the gamma radiation counts (Barbosa et al., 2017). Furthermore, the wind is predominantly blowing from the ocean (NW direction) around this seismic event, which would have prevented eventual radon transport from inland Graciosa. The ML4.2 and ML3.9 earthquakes on June 14th, the ML4.0 earthquake on June 30th, the ML3.5 event on the 4th of July and the ML4.5 event on September 26th are not associated with anomalies in gamma radiation. Overall, there is little to no evidence for an association between seismic events and gamma radiation anomalies for the considered earthquakes occurring in this area. This suggests that an alternative explanation for the observed decrease in the level of gamma radiation after August 26th is required.

3.3. Soil moisture

Soil water content is well known to influence gamma radiation measurements via attenuation of the propagation of gamma rays from the subsurface (e.g. Beamish (2013, 2015)). However, the influence of soil water content is considered to be associated with long time scales, typically of several weeks and longer (Minato, 1980; Yoshioka, 1994) and thus it seemed unlikely that an abrupt variation as the one observed in gamma radiation on 26th August 2015 could be related to soil moisture effects. However, the inspection of the available time series of soil moisture from the ENA site (Figure 6) shows an abrupt change from dry to wet conditions on August 26th 2015. This is confirmed by the Mann-Whitney test for breakpoint detection, which identifies a shift in the soil moisture time series at 5 cm and 10 cm depths on August 16th, and a day later for soil moisture at the deeper level (15 cm). After the abrupt transition in August from predominantly dry to wet conditions, the soil moisture remains at a comparatively stable and higher level, which is consistent with the lower average level of total gamma radiation until the end of 2015.

The relationship between daily-averaged soil moisture (at 5 cm) and gamma radiation counts is displayed in Fig. 7. In order to remove the influence of increased gamma radiation due to radon progeny on the ground due to rainfall, the daily averages were computed from the 15-minute gamma radiation counts by excluding all radiation measurements coincident and within 3 hours following precipitation events with an intensity larger than 1 mm/hour. As expected, higher soil moisture is associated with lower gamma counts, with a larger dispersion in the case of dry conditions. Although the relationship is nonlinear, as indicated in Fig. 7 (dashed line) by the fitted local regression curve (Cleveland, 1979), a linear model seems nevertheless a fair approximation (solid line in Fig. 7). In fact, a simple linear regression is able to explain 66% of the variability in daily gamma radiation as a function of daily soil moisture at 5 cm depth.

Figure 8 displays the time series of daily gamma radiation counts resulting from the subtraction of counts associated with soil moisture as predicted from the fitted linear model based on daily averaged soil moisture at 5 cm depth. This time series corrected for atmospheric (precipitation > 1 mm/hour) and surface (soil moisture) effects shows no sharp discontinuities.

4. Discussion

Diverse geoscience applications of gamma radiation measurements involve the identification of anomalies that could be associated with the process of interest, such as tectonic activity or fluid migration (Barbosa et al., 2015). It is then crucial to identify confounding factors, such as meteorological effects related to pressure and temperature (e.g. Zafrir et al. (2013)) or strong rainfall events (e.g. Greenfield et al. (2002)). Understanding the anomalies in time series of environmental radioactivity is particularly critical for assessing potential earthquake precursors. The task is hindered by the similarity of anomalies of meteorological or hydrological origin and of anomalies of seismic origin, since the underlying physical mechanism - mixing ratio change between different fluid end-members driven by pressure changes in one end-member - can be the same (Woith, 2015).

Soil moisture is well known to affect gamma radiation (e.g. Szegvary et al. (2007); Stöhlker et al. (2012)), but typically the effect is expected to be approximately linear and to take place on long time scales of weeks or longer. At the ENA site, the temporal variability of soil moisture is strongly non-linear, with very fast (< 1 day) transitions from dry to wet conditions. This pattern results from the specific volcanic soil type and climatic conditions of the island. In the flat northern platform of Graciosa island where the ENA station is located, the soil thickness is typically small and porosity is high (Medina & Grilo, 1981). The volcanic origin and sandy nature of the soil leads to high evaporation and quick infiltration, resulting in the alternating behavior of soil moisture between low values in the summer and high values in winter, with an abrupt transition between the two states. In 2015, the transition from dry to wet conditions was very abrupt and persisted in time (for several months) leading to a discontinuous pattern in the time series of gamma radiation.

Soil moisture affects gamma radiation through the attenuation of photons from terrestrial radionuclides, and thus gamma radiation measurements may reflect both sharp and slow soil moisture variations. Figure 9 shows the predicted daily gamma radiation based on the linear relationship between gamma radiation and soil moisture derived in section 3.4. Although the model is very simple, it is able to capture the main features of the gamma radiation time series for the year 2015 using only the available soil moisture information at 5 cm depth. Fig. 9 also shows the predicted gamma radiation for the first-half of 2016 using the same model. This provides an independent assessment of the performance of the model since the parameters of the linear regression were estimated using only the gamma radiation and soil moisture measurements from 2015. The predicted gamma radiation for 2016 agrees reasonably well with the observed values in the first months of the year, but the predictions become progressively worse after May 2016. This is hardly surprising since the model is very poor for dry conditions, as indicated by the very large dispersion for low soil moisture in Fig. 7. Nevertheless, the model predictions provide a very reasonable representation of long-term variability of gamma radiation for the winter period based only on soil moisture at 5 cm depth for time scales of days to several weeks.

Figure 10 displays all the currently available soil moisture and gamma radiation measurements from the ENA site (since May 2015 to the end of August 2018). Clearly, the seasonal variability of soil moisture is not fully reflected in the gamma radiation measurements, although on average high soil moisture values tend to be associated with lower gamma radiation. There are at least two obvious reasons for this. First, near-surface gamma radiation not only depends on terrestrial radiation from decaying radioisotopes within the soil, but is also affected by cosmic radiation. At seasonal and longer time scales, variations in background cosmic radiation need to be considered. Second, the vertical distribution of soil moisture in the top soil needs to be considered since a single measurement at 5 cm depth is likely not representative for the entire top soil affecting terrestrial gamma radiation. To make significant progress in understanding how soil moisture dynamics affects gamma radiation, a more elaborate modeling strategy combining depth-resolved hydrological models (Vereecken et al., 2015) and models for incoming and terrestrial gamma radiation would be needed, which is clearly beyond the scope of this manuscript.

It is important to emphasize that the obtained relationship between gamma radiation and soil moisture is site- and equipment-specific. As already shown by Beamish (2013), soil porosity is known to have a strong effect on this relationship. More importantly, attenuation of gamma radiation by soil moisture is known to be energy-dependent, which means that the relationship between gamma radiation and soil moisture will depend on the measured energy spectra. Finally, the soil moisture measurements were normalized before further processing, which was necessary due to the rather primitive soil moisture sensors used at the ENA site (intended as a support to surface energy balance measurements rather than for the specific measurement of soil moisture). Future studies should consider the use of state-of-the-art soil moisture sensors, which are increasingly available at low cost (e.g. Bogena et al. (2017)).

5. Conclusions

The present study shows that abrupt changes in soil moisture can cause sharp variations in total gamma radiation measurements that can be confused with an earthquake precursory indicator. Therefore, soil moisture effects need to be taken into account to reduce the number of false positives in earthquake precursory studies (i.e., the cases when an anomaly exists but is not related to an earthquake event). It is thus fundamental to carefully assess not only meteorological conditions, particularly precipitation, but also surface conditions, particularly soil moisture. High-resolution (sub-hourly) measurements of these parameters, as available at the ENA station, are critical to discriminate atmospheric and surface effects, as precipitation and soil moisture are not independent and temporal averaging blurs the attribution of the sources of variability in gamma radiation.

Acknowledgments

The invaluable technical assistance of Mr Carlos Sousa, Mr Bruno Cunha and Mr Tércio Silva from the ARM-ENA facility is gratefully acknowledged. Data were obtained from the Atmospheric Radiation Measurement (ARM) Program sponsored by the U.S. Department of Energy, Office of Science, Office of Biological and Environmental Research, Climate and Environmental Sciences Division. This work is partially supported by Project "Coral - Sustainable Ocean Exploitation: Tools and Sensors/NORTE-01-0145-FEDER-000036", financed by the North Portugal Regional Operational Programme (NORTE 2020) under the PORTUGAL 2020 Partnership Agreement and by the European Regional Development Fund (ERDF). Support from project POCI-01-0145-FEDER-006961 financed by the Operational Programme for Competitiveness and Internationalisation - COMPETE 2020, and National Funds through the FCT Fundação para a Ciência e a Tecnologia is also acknowledged.

References

Arora, B. R., Kumar, A., Walia, V., Yang, T. F., Fu, C.-C., Liu, T.-K., Wen, K.-L., & Chen, C.-H. (2017). Assesment of the response of the meteorological/hydrological parameters on the soil gas radon emission at Hsinchu, northern Taiwan: A prerequisite to identify earthquake precursors. *Journal of Asian Earth Sciences*, *149*, 49–63.

Azevedo, E. (2015). O clima dos Açores - Projecto CLIMAAT - Centro do Clima, Meteorologia e Mudanças Globais da Universidade dos Açores. Http://www.climaat.angra.uac.pt/.

Barbosa, S., Donner, R., & Steinitz, G. (2015). Radon applications in geosciences - Progress & perspectives. *The European Physical Journal Special Topics*, *224*, 597–603.

Barbosa, S., Mendes, V. B., & Azevedo, E. B. (2016). Radon progeny monitoring at the Eastern North Atlantic (ENA), Graciosa island ARM facility and a potential earthquake precursory signal. In *EGU General Assembly Conference Abstracts* (p. 6270). volume 18.

Barbosa, S., Miranda, P., & Azevedo, E. (2017). Short-term variability of gamma radiation at the {ARM} Eastern North Atlantic facility (Azores). *Journal of Environmental Radioactivity*, *172*, 218–231.

Beamish, D. (2013). Gamma ray attenuation in the soils of Northern Ireland, with special reference to peat. *Journal of Environmental Radioactivity*, *115*, 13–27.

Beamish, D. (2015). Relationships between gamma-ray attenuation and soils in SW England. *Geoderma*, *259-260*, 174–186.

Bogena, H. R., Huisman, J. A., Schilling, B., Weuthen, A., & Vereecken, H. (2017). Effective calibration of low-cost soil water content sensors. *Sensors*, *17*, 208.

Bossew, P., Cinelli, G., Hernndez-Ceballos, M., Cernohlawek, N., Gruber, V., Dehandschutter, B., Menneson, F., Bleher, M., Sthlker, U., Hellmann, I., Weiler, F., Tollefsen, T., Tognoli, P., & de Cort, M. (2017). Estimating the terrestrial gamma dose rate by decomposition of the ambient dose equivalent rate. *Journal of Environmental Radioactivity*, *166*, 296–308.

Carroll, T. R. (1981). Airborne soil moisture measurement using natural terrestrial gamma radiation. *Soil Science*, *132*, 358–366.

Chambers, S., Williams, A., Zahorowski, W., Griffiths, A., & Crawford, J. (2011). Separating remote fetch and local mixing influences on vertical radon measurements in the lower atmosphere. *Tellus B: Chemical and Physical Meteorology*, *63*, 843–859.

Cleveland, W. S. (1979). Robust Locally Weighted Regression and Smoothing Scatterplots. *Journal of the American Statistical Association*, *74*, 829–836.

Cook, D. R. (2016). Surface energy balance system (sebs) handbook. Doi: 10.2172/1245980.

Fu, C.-C., Wang, P.-K., Lee, L.-C., Lin, C.-H., Chang, W.-Y., Giuliani, G., & Ouzounov, D. (2015). Temporal variation of gamma rays as a possible precursor of earthquake in the longitudinal valley of eastern taiwan. *Journal of Asian Earth Sciences*, *114*, 362 – 372.

Girault, F., Schubnel, A., & Pili, E. (2017). Transient radon signals driven by fluid pressure pulse, micro-crack closure, and failure during granite deformation experiments. *Earth and Planetary Science Letters*, *474*, 409 – 418.

Greenfield, M. B., Domondon, A. T., Okamoto, N., & Watanabe, I. (2002). Variation in -ray count rates as a monitor of precipitation rates, radon concentrations, and tectonic activity. *Journal of Applied Physics*, *91*, 1628–1633.

Hildenbrand, A., Weis, D., Madureira, P., & Marques, F. O. (2014). Recent plate re-organization at the Azores Triple Junction: Evidence from combined geochemical and geochronological data on Faial, S. Jorge and Terceira volcanic islands. *Lithos*, *210-211*, 27–39.

Hipólito, A., Madeira, J., Carmo, R., & Gaspar, J. a. L. (2014). Neotectonics of Graciosa island (Azores): a contribution to seismic hazard assessment of a volcanic area in a complex geodynamic setting. *Annals of Geophysics*, *56*.

Holub, R., & Brady, B. (1981). The effect of stress on radon emanation from rock. *Journal of Geophysical Research: Solid Earth*, *86*, 1776–1784.

Inomata, Y., Chiba, M., Igarashi, Y., Aoyama, M., & Hirose, K. (2007). Seasonal and spatial variations of enhanced gamma ray dose rates derived from 222Rn progeny during precipitation in Japan. *Atmospheric Environment*, *41*, 8043–8057.

Jordan, T., Chen, Y.-T., Gasparini, P., Madariaga, R., Main, I., Marzocchi, W., Papadopoulos, G., Yamaoka, K., Zschau, J. et al. (2011). Operational earthquake forecasting: State of knowledge and guidelines for implementation. *Annals of Geophysics*, *54*, 315–391.

Livesay, R., Blessinger, C., Guzzardo, T., & Hausladen, P. (2014). Rain-induced increase in background radiation detected by Radiation Portal Monitors. *Journal of Environmental Radioactivity*, *137*, 137–141.

Madruga, J., Azevedo, E. B., Sampaio, J. F., Fernandes, F., Reis, F., & Pinheiro, J. (2015). Analysis and definition of potential new areas for viticulture in the Azores (Portugal). *SOIL*, *1*, 515–526.

Medina, J. B., & Grilo, J. T. (1981). *Esboço pedológico da ilha Graciosa (Açores)*. Instituto Nacional de Investigação Científica.

Melintescu, A., Chambers, S., Crawford, J., Williams, A., Zorila, B., & Galeriu, D. (2018). Radon-222 related influence on ambient gamma dose. *Journal of Environmental Radioactivity*, *189*, 67–78.

Mercier, J.-F., Tracy, B., d'Amours, R., Chagnon, F., Hoffman, I., Korpach, E., Johnson, S., & Ungar, R. (2009). Increased environmental gamma-ray dose rate during precipitation: a strong correlation with contributing air mass. *Journal of Environmental Radioactivity*, *100*, 527–533.

Minato, S. (1980). Analysis of Time Variations in Natural Background Gamma Radiation Flux Density. *Journal of Nuclear Science and Technology*, *17*, 461–469.

Mollo, S., Tuccimei, P., Heap, M., Vinciguerra, S., Soligo, M., Castelluccio, M., Scarlato, P., & Dingwell, D. B. (2011). Increase in radon emission due to rock failure: An experimental study. *Geophysical Research Letters*, *38*.

Nicolas, A., Girault, F., Schubnel, A., Pili, É., Passelègue, F., Fortin, J., & Deldicque, D. (2014). Radon emanation from brittle fracturing in granites under upper crustal conditions. *Geophysical Research Letters*, *41*, 5436–5443.

Nitschke, K., & de Azevedo, E. B. (2015). 3d atmosphere column evaluation and clouds tomography: At eastern north atlantic (ena), graciosa island arm facility. In *Experiment@ International Conference (exp. at'15), 2015 3rd* (pp. 91–92). IEEE.

Novikov, A., Ulin, S., Dmitrenko, V., Vlasik, K., Bychkova, O., Petrenko, D., Uteshev, Z., & Shustov, A. (2016). Measurement of radon concentration by xenon gamma-ray spectrometer for seismic monitoring of the earth. *Journal of Physics: Conference Series*, *675*, 042007.

Paatero, J., & Hatakka, J. (1999). Wet deposition efficiency of short-lived radon-222 progeny in central Finland. *Boreal Env. Res.*, *4*, 285–293.

Ross, G. (2015). Parametric and Nonparametric Sequential Change Detection in R: The cpm Package. *Journal of Statistical Software*, *66*, 1–20.

Stöhlker, U., Bleher, M., Conen, F., & Bänninger, D. (2012). Harmonization of ambient dose rate monitoring provides for large scale estimates of radon flux density and soil moisture changes. *Proceedings Series*, (p. 53).

Szegvary, T., Conen, F., Sthlker, U., Dubois, G., Bossew, P., & de Vries, G. (2007). Mapping terrestrial gamma-dose rate in europe based on routine monitoring data. *Radiation Measurements*, *42*, 1561 – 1572.

Tsvetkova, T., Monnin, M., Nevinsky, I., & Perelygin, V. (2001). Research on variation of radon and gamma-background as a prediction of earthquakes in the caucasus. *Radiation Measurements*, *33*, 1 – 5.

Tsvetkova, T., Nevinsky, I., & Nevinsky, V. (2014). Results of spectral monitoring of environmental gamma background in a fault zone of the western caucasus for seismological application. *Radiation Measurements*, *69*, 35 – 49.

Vereecken, H., Huisman, J.-A., Franssen, H. H., Brüggemann, N., Bogena, H. R., Kollet, S., Javaux, M., van der Kruk, J., & Vanderborght, J. (2015). Soil hydrology: Recent methodological advances, challenges, and perspectives. *Water resources research*, *51*, 2616–2633.

Vogt, P., & Jung, W. (2004). The terceira rift as hyper-slow, hotspot-dominated oblique spreading axis: a comparison with other slow-spreading plate boundaries. *Earth and Planetary Science Letters*, *218*, 77–90.

Woith, H. (2015). Radon earthquake precursor: A short review. *The European Physical Journal Special Topics*, *224*, 611–627.

Yakovleva, V. S., Nagorsky, P. M., Cherepnev, M. S., Kondratyeva, A. G., & Ryabkina, K. S. (2016). Effect of precipitation on the background levels of the atmospheric beta- and gamma-radiation. *Applied Radiation and Isotopes*, *118*, 190–195.

Yoshioka, K. (1994). Study of Time Variation of Terrestrial Gamma Radiation Due to Depth Distribution of Soil Moisture Content. *Radioisotopes*, *43*, 183–189.

Zafrir, H., Barbosa, S. M., & Malik, U. (2013). Differentiation between the effect of temperature and pressure on radon within the subsurface geological media. *Radiation Measurements*, *49*, 39–56.

Zafrir, H., Haquin, G., Malik, U., Barbosa, S., Piatibratova, O., & Steinitz, G. (2011). Gamma versus alpha sensors for Rn-222 long-term monitoring in geological environments. *Radiation Measurements*, *46*, 611–620.

List of figures

Figure 1: Geographical location of the gamma radiation monitoring campaign at the Graciosa Island, Azores (top) and detail of the Eastern North Atlantic (ENA) ARM site (bottom). Soil moisture is obtained from SEBS (Surface Energy Balance System) measurements, at a distance of 130m from the gamma measurements.

Figure 2: Time series of total gamma counts in counts per minute (cpm), every 15 minutes from 2015-05-08 to 2015-12-31. The vertical dashed line marks the time of the shift in the time series as identified by the Mann-Whitney test.

Figure 3: Detail of the time series of gamma counts (in cpm) and precipitation rate (in mm/hour) for the period around the identified break-point on 2015/08/26 02:45. Wind information (mean speed and wind direction) is displayed for the same period on the top right.

Figure 4: Map with the locations of all earthquakes in the Azores region from 2015/05/08 to 2015/12/31. The ML3.3 earthquake on 2015/08/26 is marked by an X.

Figure 5: Detail of the time series of gamma counts (in cpm) and precipitation rate (in mm/hour) around the largest earthquake events (the dashed vertical line indicates the time of occurrence of the earthquake). Wind information (mean speed and wind direction) is shown on the top left side.

Figure 6: Time series of soil moisture values every 30-minutes (points) and daily averaged (black line) at 5cm (top), 10 cm (middle) and 15 cm (bottom) depths.

Figure 7: Scatter-plot of daily values of soil moisture (at 5 cm depth) and gamma radiation for the year 2015. The daily averages are computed excluding all the measurements coincident and within the following 3 hours of precipitation events with intensity larger than 1 mm/hour.

Figure 8: Time series of daily gamma counts after correction for the soil moisture influence using the fitted linear model (solid dark line) superimposed on the original time series of gamma measurements as in Fig. 2 (gray).

Figure 9: Time series of daily soil moisture (top) and gamma counts (bottom, grey) along with gamma counts from the fitted linear model for the year 2015 (solid line, dark blue) and predictions from the model for the first half of 2016 (dashed line, light blue).

Figure 10: Time series of weekly averaged soil moisture (top) and gamma counts (bottom) from May 2015 to the end of August 2018.

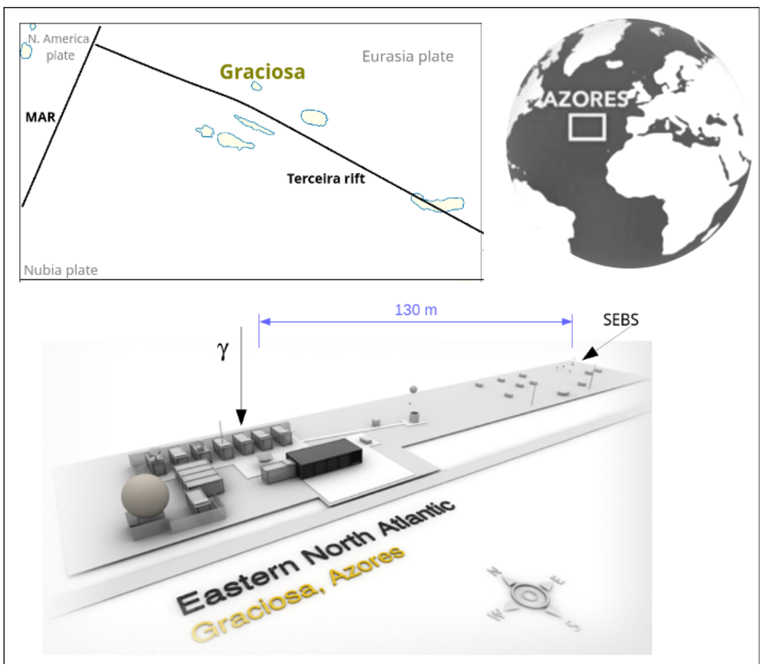

Figure 1: Geographical location of the gamma radiation monitoring campaign at the Graciosa Island, Azores (top) and detail of the Eastern North Atlantic (ENA) ARM site (bottom). Soil moisture is obtained from SEBS (Surface Energy Balance System) measurements, at a distance of 130m from the gamma measurements.

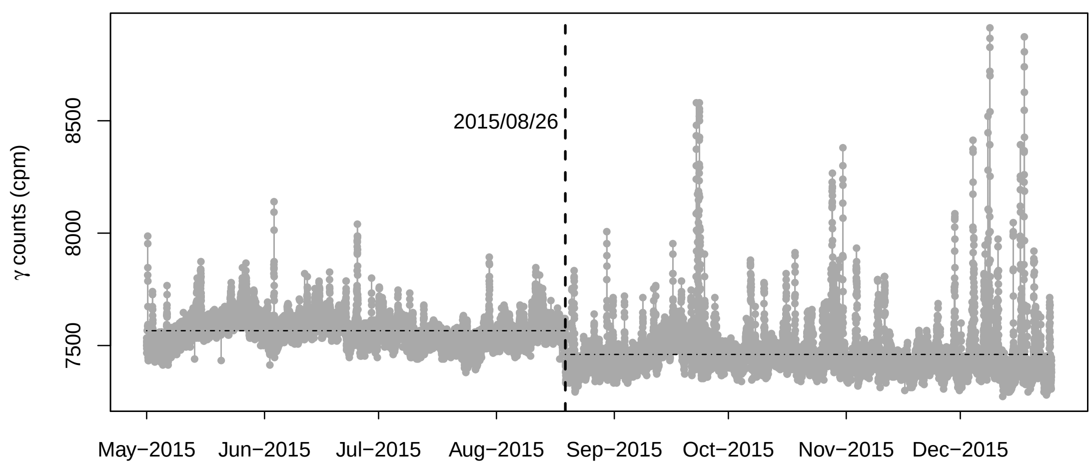

Figure 2: Time series of total gamma counts in counts per minute (cpm), every 15 minutes from 2015-05-08 to 2015-12-31. The vertical dashed line marks the time of the shift in the time series as identified by the Mann-Whitney test.

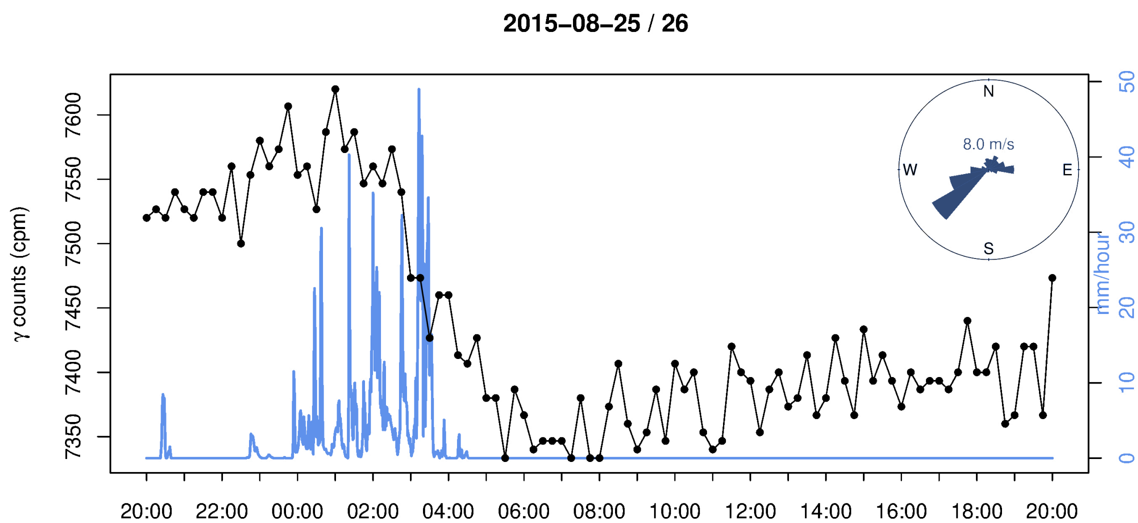

Figure 3: Detail of the time series of gamma counts (in cpm) and precipitation rate (in mm/hour) for the period around the identified break-point on 2015/08/26 02:45. Wind information (mean speed and wind direction) is displayed for the same period on the top right.

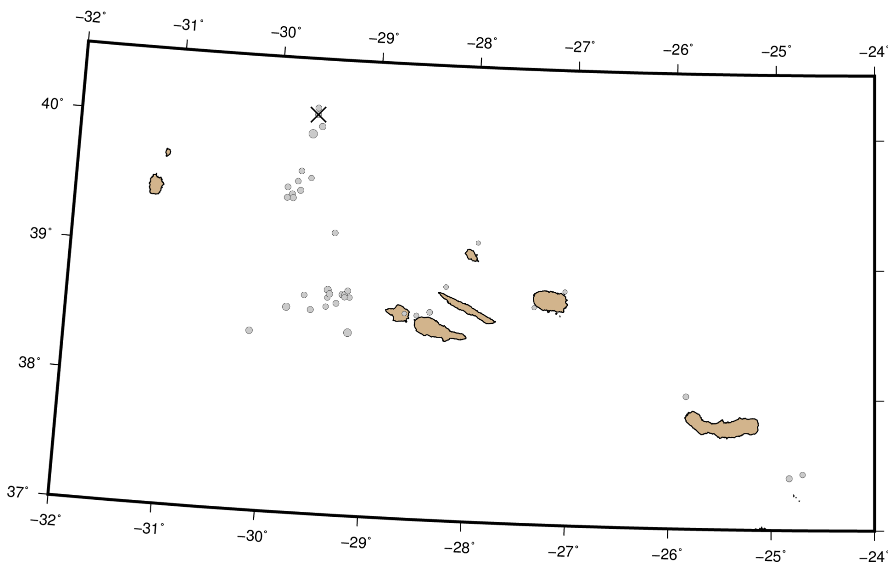

Figure 4: Map with the locations of all earthquakes in the Azores region from 2015/05/08 to 2015/12/31. The ML3.3 earthquake on 2015/08/26 is marked by an X.

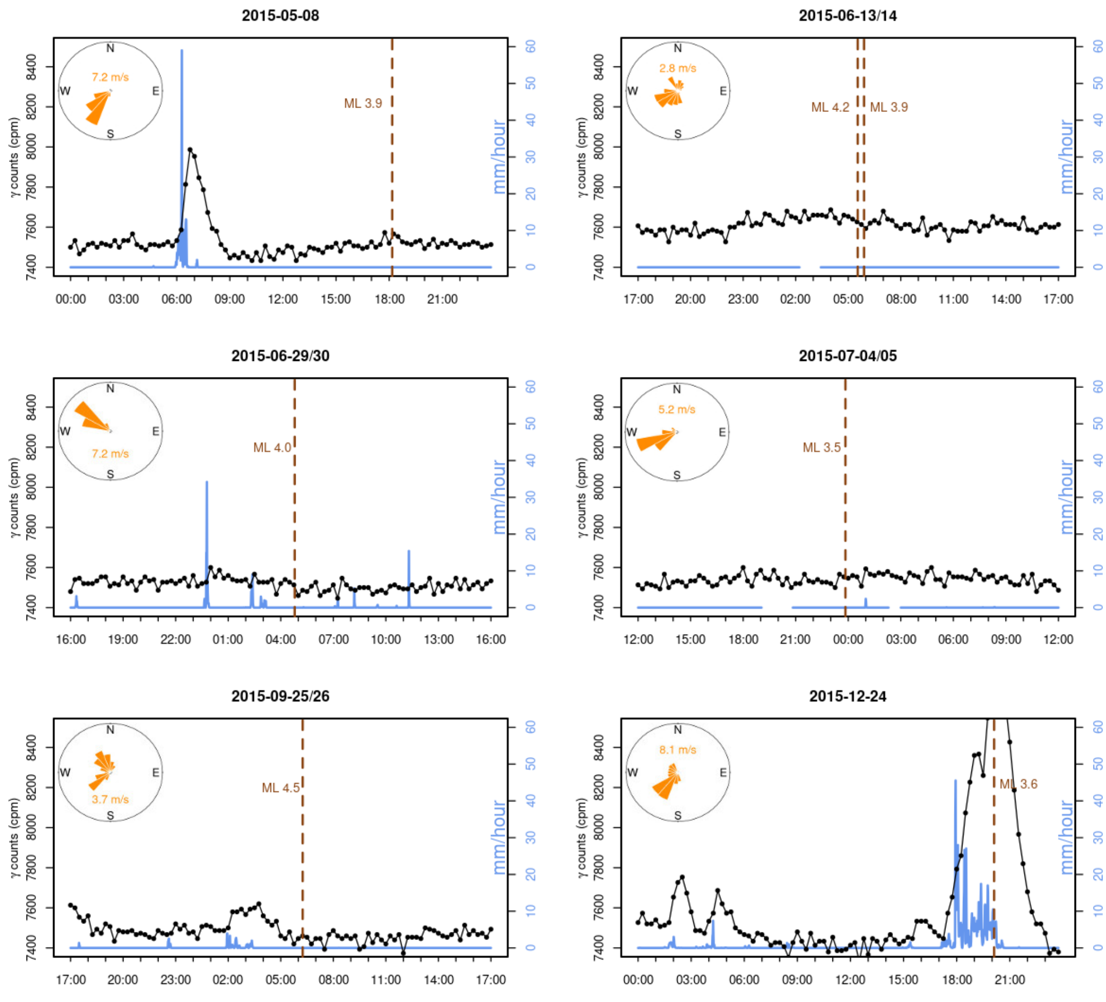

Figure 5: Detail of the time series of gamma counts (in cpm) and precipitation rate (in mm/hour) around the largest earthquake events (the dashed vertical line indicates the time of occurrence of the earthquake). Wind information (mean speed and wind direction) is shown on the top left side.

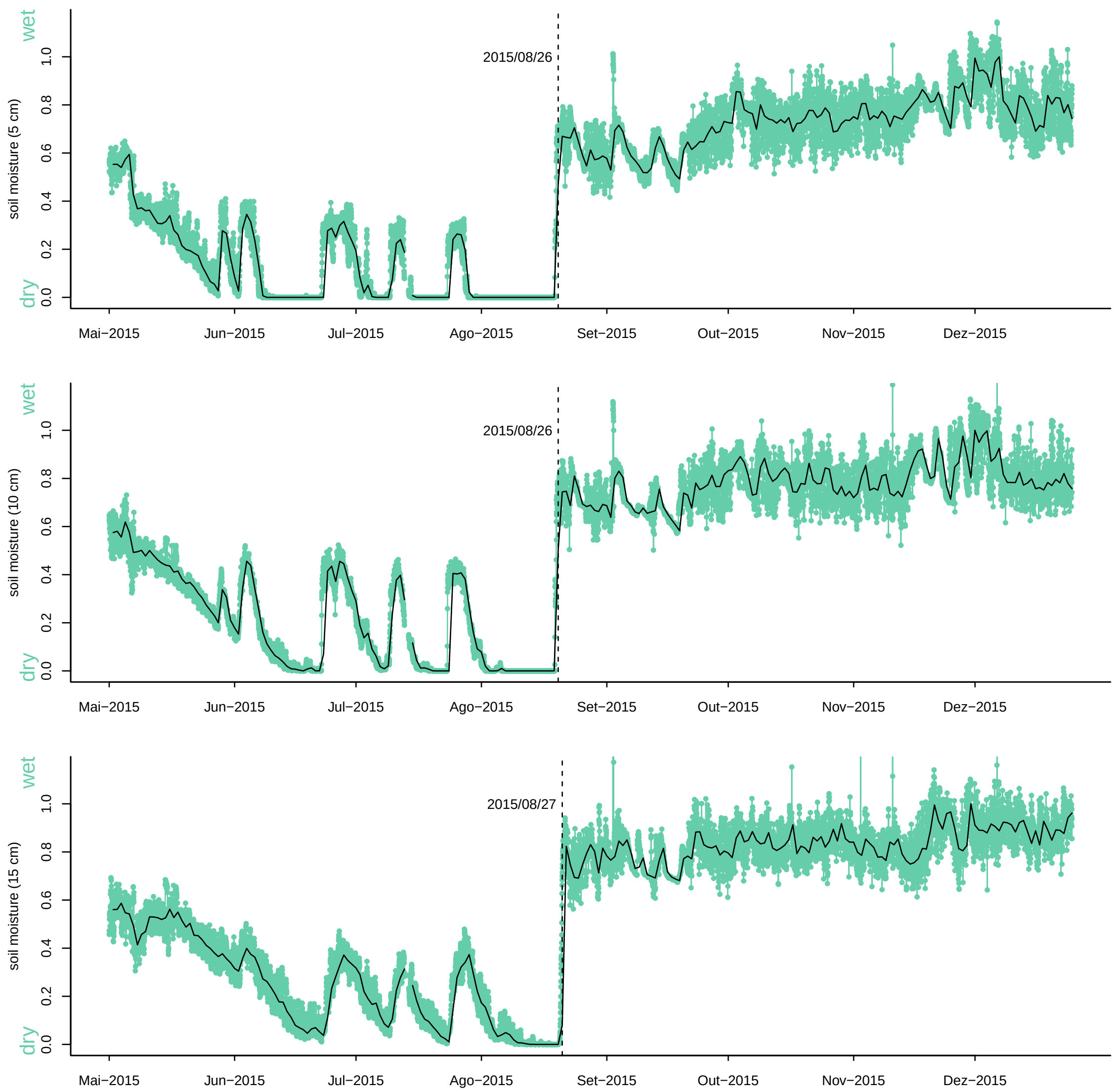

Figure 6: Time series of soil moisture values every 30-minutes (points) and daily averaged (black line) at 5cm (top), 10 cm (middle) and 15 cm (bottom) depths.

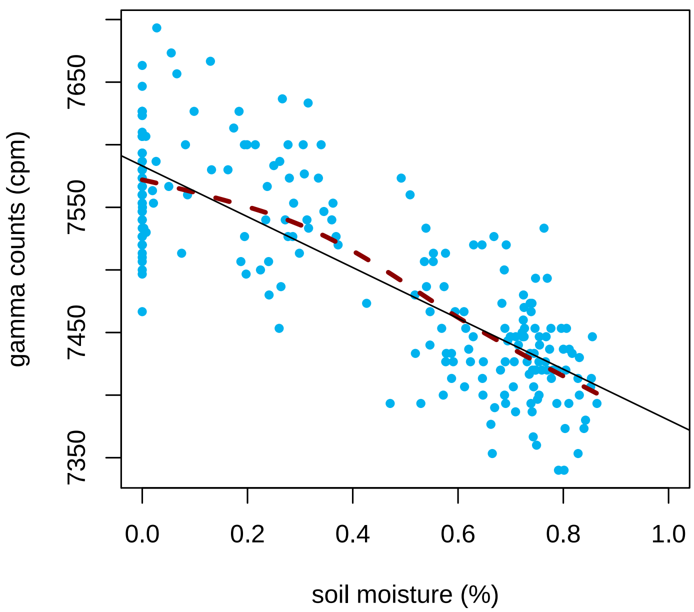

Figure 7: Scatter-plot of daily values of soil moisture (at 5 cm depth) and gamma radiation for the year 2015. The daily averages are computed excluding all the measurements coincident and within the following 3 hours of precipitation events with intensity larger than 1 mm/hour.

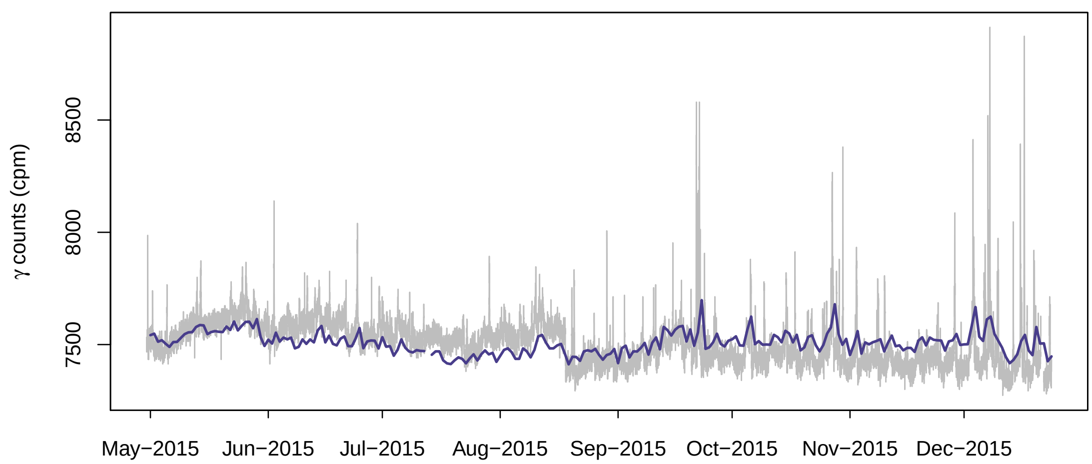

Figure 8: Time series of daily gamma counts after correction for the soil moisture influence using the fitted linear model (solid dark line) superimposed on the original time series of gamma measurements as in Fig. 2 (gray).

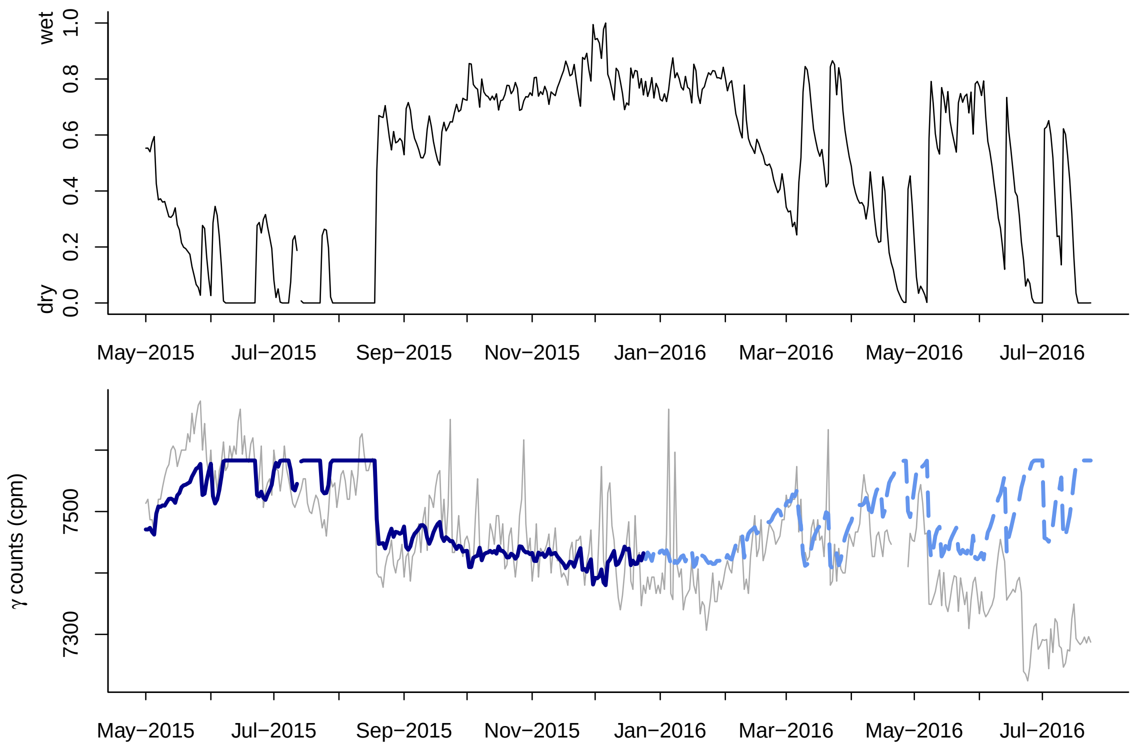

Figure 9: Time series of daily soil moisture (top) and gamma counts (bottom, grey) along with gamma counts from the fitted linear model for the year 2015 (solid line, dark blue) and predictions from the model for the first half of 2016 (dashed line, light blue).

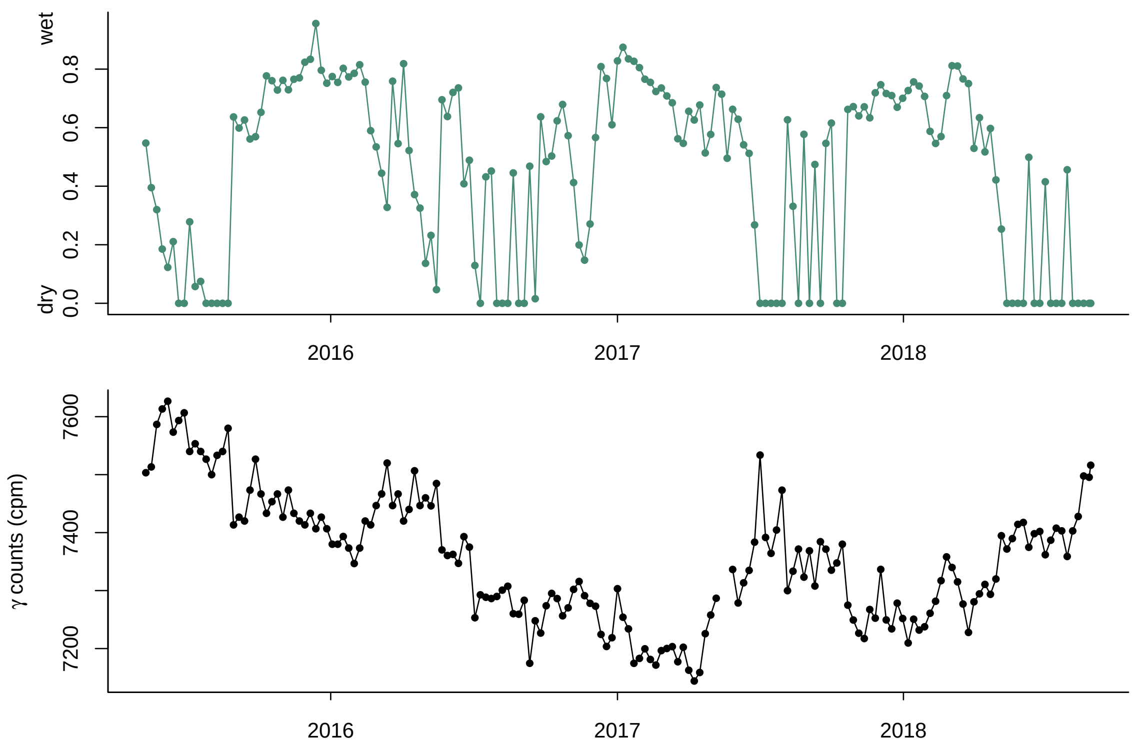

Figure 10: Time series of weekly averaged soil moisture (top) and gamma counts (bottom) from May 2015 to the end of August 2018.